JOURNAL OF SOLID STATE CHEMISTRY 76, 210–217 (1988)

Phase Diagram, Optical Energy Gap, and Magnetic Susceptibility of $(CuGa)_{1-z}Mn_{2z}Te_2$ Alloys

M. QUINTERO, P. GRIMA, AND R. TOVAR

Centro de Estudios de Semiconductores, Departamento de Física, Universidad de los Andes, Mérida, Venezuela

AND R. GOUDREAULT, D. BISSONNETTE, G. LAMARCHE, AND J. C. WOOLLEY

Ottawa-Carleton Institute of Physics, University of Ottawa, Ottawa, Ontario, Canada K1N 6N5

Received March 21, 1988

Polycrystalline samples of $(CuGa)_{1-z}Mn_{2z}Te_2$ alloys were prepared by the melt and anneal technique and were used in differential thermal analysis, lattice parameter, optical energy gap, and magnetic susceptibility measurements. It was found that in the equilibrium diagram the range of single-phase solid solution at room temperature is very small with the chalcopyrite phase existing for $0 \leq z \leq 0.04$ and no zinc blende phase occurring. However, above 600°C, the chalcopyrite and zinc blende phases together show single-phase behavior out to $z = 0.4$. Samples water-quenched from 650°C were found to be predominantly metastable manganese-ordered zinc blende. Thus the optical and magnetic data for this phase can be obtained and is in good agreement with the values obtained previously for other chalcopyrite-derived semimagnetic semiconductors.

Introduction

Semiconductor alloys containing paramagnetic manganese ions are of interest because of their magnetic as well as semiconductor properties. Pseudobinary alloys of the form $II_{1-z}Mn_zVI$, such as $Cd_{1-z}Mn_zTe$, have been investigated in much detail (*1–4*) and the work has been extended to pseudoternary alloys such as $Cd_xZn_yMn_zTe$ $(x + y + z = 1)$ (e.g., (*5, 6*)). In all of these alloys, the manganese ions are arranged at random on the cation sublattice and as a result the alloys show spin-glass behavior at low temperatures. These alloys have been given the names semimagnetic semiconductor or diluted magnetic semiconductor alloys. Other possible semimagnetic alloys can be derived from the chalcopyrite I III VI_2 compounds, the ternary analogs of the II VI compounds. To retain the electron to atom ratio and hence the semiconductor properties, it is necessary to replace one I and one III cation simultaneously by two manganese atoms, so that the alloys of interest have the form $(I\ III)_{1-z}Mn_{2z}Te_2$ or in the more general pseudoternary case $II_{2x}(I\ III)_yMn_{2z}Te_2$ $(x + y + z = 1)$.

Lattice parameter and optical energy gap

0022-4596/88 $3.00

data have been obtained for the systems $Cd_{2x}(CuIn)_yMn_{2z}Te_2$ (*7*) and $Cd_{2x}(AgIn)_yMn_{2x}Te_2$ (*8*) and magnetic measurements made on various $(I\ III)_{1-z}Mn_{2z}Te_2$ alloys (*9*). The results indicate that ordering of the manganese ions on the cation sublattice occurs in these alloys and that this has a significant effect on the magnetic behavior and on the optical energy gap values. In order to examine these effects in more detail, it is necessary to have information concerning the phase diagram and the ordered structure of those alloys. In recent work, DTA measurements were made to give the $T(z)$ phase diagrams of the $(CuIn)_{1-z}Mn_{2z}Te_2$ (*10, 11*), $(AgIn)_{1-z}Mn_{2z}Te_2$ (*11*), and $(AgGa)_{1-z}Mn_{2z}Te_2$ (*12*) systems. In all cases, it was found that single-phase solid solution was obtained from $z = 0$ to at least $z = 0.5$ down to room temperature, the single phase being either the zinc blende or the chalcopyrite structure. In addition, in these structures ordering of the Mn atoms on the cation sublattice was observed at lower temperatures, ordering temperatures of up to 450°C being found. It also has been shown that Mn ordering in either the zinc blende or the chalcopyrite structure has negligible effect on the lattice parameter values, but that the optical energy gap E_0 values in the Mn-ordered and Mn-disordered alloys are appreciably different. In addition, the magnetic behavior of these two phases is very different as indicated by the values of the magnetic transition temperatures T_m (*9*), which are attributed to paramagnetism–spin-glass transitions. Thus measurements of optical energy gap and the temperature variation of magnetic susceptibility give very useful information to supplement the DTA and lattice parameter data.

In the case of $(CuGa)_{1-z}Mn_{2z}Te_2$ alloys, little information has been given. Aresti *et al.* (*10*) have indicated that solubility of MnTe in $CuGaTe_2$ is limited to $z = 0.05$. However, the present authors (*9*) have indicated that, with relatively random quenching conditions, a few samples under single-phase condition have been obtained out to $z = 0.4$. In the present work, measurements of DTA, lattice parameter, optical energy gap, and magnetic susceptibility have been made to give a clearer presentation of the $T(z)$ diagram of the $(CuGa)_{1-z}Mn_{2z}Te_2$ alloys.

Experimental Methods

Polycrystalline samples of the alloys were prepared by the melt and anneal technique (*7*). To reduce the problems of working with gallium, the compound Ga_2Te_3 was prepared first and then alloy samples were made from the appropriate weights of Cu, Mn, Te, and Ga_2Te_3. The appropriate annealing temperature was uncertain until the $T(z)$ diagram was determined, and annealing at 600°C for about 20 days followed by slow cooling to room temperature was used to give samples for the DTA measurements. (With the furnace switched off at 600°C, cooling to room temperature took about 10 hr.) The DTA data indicated that 600°C was probably not a good choice for annealing temperature, but samples annealed at other temperatures were found to give the same DTA data. However, annealing at other temperatures was necessary for the samples for lattice parameter, optical energy gap, and magnetic susceptibility measurements. These will be mentioned below in the relevant places. For all samples prepared, powder X-ray photographs, either Debye–Scherrer or Guinier, were taken to determine the phase condition and lattice parameter values for any zinc blende or chalcopyrite phase obtained.

Differential thermal analysis measurements (*13*) were made for a range of sample compositions, with 50–100 mg specimens being used. Since the work was part of a program for the investigation of semimagnetic semiconductor alloys, the range of

composition investigated was limited to $0 \leq z \leq 0.7$ and the behavior of the Mn-rich phases was not considered. Thus a maximum temperature of 1000°C was sufficient for the work and silver was used as the reference material. Heating and then cooling runs were carried out on each sample investigated.

Room temperature optical energy gap (E_0) values were measured by the usual optical absorption method (*14*). For each sample, a slice was polished down to a thickness d in the range 40–100 μm. The variations of I_0, the intensity of the incident radiation, and I_t, the transmitted intensity, were determined as a function of photon energy $h\nu$ and values of $1/d \ln I_0/I_t$ found. These values were corrected by subtracting a background value to give the absorption coefficient α and the relation $\alpha h\nu = A(E_0 - h\nu)^{1/2}$ was then used to give a value for E_0.

Magnetic susceptibility (χ) measurements were made using a SQUID magnetometer with magnetic fields in the range 10 to 25 G and over a temperature range 4.2 to 200 K (*15*). Peaks in the curve of χ vs T gave values of the magnetic transition temperatures, T_m.

Phase and Crystallographic Results

The results of the DTA measurements are shown by the points in Fig. 1, where heating and cooling curve data are indicated separately. The proposed phase boundaries determined from these points are shown as full lines. The dashed lines show phase boundaries estimated with the help of X-ray and optical energy gap results. In Fig. 1, the values at $z = 0$, i.e., $CuGaTe_2$, are in good agreement with the results of Congiu *et al.* (*16*) for the $CuGaTe_2$ point in the Cu_2Te–Ga_2Te_3 diagram. In the present work, α is the chalcopyrite phase, β the zinc blende phase, and γ the hexagonal NiAs structure of MnTe. As seen from the diagram of Congiu *et al.*, two different zinc blende fields are present, accounting for the β and β_1 phases in the present work. Also from that diagram, η is a Cu_2Te-rich hexagonal phase. Finally, by comparison with the $(CuIn)_{1-z}Mn_{2z}Te_2$ diagram (*10*), δ has the rock salt structure shown by MnTe above 1050°C, but which exists at lower temperatures elsewhere in the general diagram. The present section is clearly not completely pseudobinary.

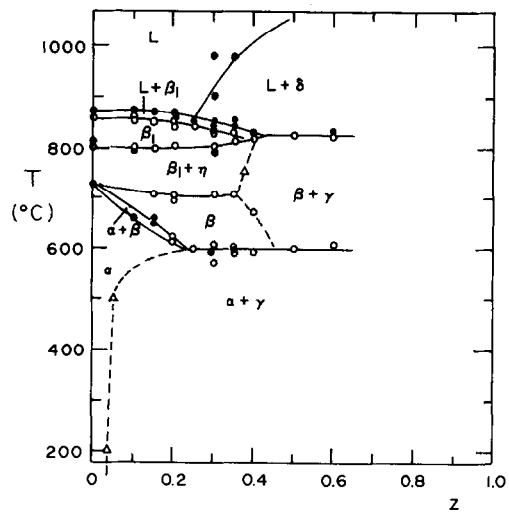

FIG. 1. $T(z)$ diagram for $(CuGa)_{1-z}Mn_{2z}Te_2$ alloys. DTA: ○, heating run; ●, cooling run; △, from lattice parameter data.

As is seen from Fig. 1, it was not possible to determine the boundary between the α and $(\alpha + \gamma)$ fields from DTA data. Therefore samples were annealed at various temperatures and water quenched to retain as much as possible the equilibrium at the annealing temperature. X-ray photographs were then used to determine structures and lattice parameter values. Values of the lattice parameter a for both the chalcopyrite and zinc blende phases are shown in Fig. 2. It was found in all chalcopyrite phases investigated that c/a had a value between 1.980 and 1.985. In Fig. 2 it is seen that all samples which were slowly cooled to 200°C were found to be two phase $(\alpha + \gamma)$, the results indicating that in this field the tie

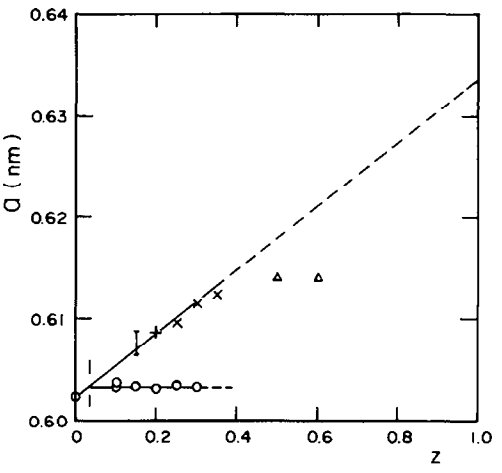

FIG. 2. Lattice parameter a vs z for $(Cu Ga)_{1-z}Mn_{2z}Te_2$ alloys. Slowly cooled samples: ○, chalcopyrite. Quenched from 650°C: +, I chalcopyrite; ×, zinc blende. Quenched from 750°C: △, zinc blende.

lines probably lie in the plane of the diagram.

To check the form of the phase diagram above 500°C, small samples (~200 mg) were annealed at 600 or at 650°C and quenched in water. Clearly such samples need not show equilibrium conditions and may be a mixture of the phases occurring in the cooling process. However, it is often possible with such samples to obtain values for lattice parameter, optical energy gap, magnetic transition temperature, etc., for a particular phase. It was found that the phase condition of the resulting samples appeared to depend critically upon the exact cooling conditions.

Samples with $z = 0.10$ and 0.15 were annealed at 600°C and quenched, in an attempt to obtain examples of the chalcopyrite phase. Both samples, although rapidly quenched, showed the two-phase ($\alpha + \gamma$) behavior characteristic of the lower temperature range but the $z = 0.15$ sample also showed faint lines corresponding to the single-phase α condition at 600°C. These lines were used to give the approximate value of a shown in Fig. 2. Various samples with $z = 0.20$, 0.25, 0.30, and 0.35 were annealed at 650°C, to be in the single-phase β field, and quenched. The samples with $z = 0.30$ and 0.35 appeared in apparently single-phase cubic form, which gave the lattice parameter values shown in Fig. 2. In the case of alloys with $z = 0.20$ and 0.25, the samples appeared to be mainly two phase ($\alpha + \gamma$) but showed also a smaller amount of the cubic β or chalcopyrite α phase corresponding to the appropriate z value. For these nonequilibrium samples, it was frequently difficult to distinguish in the X-ray photographs between zinc blende and chalcopyrite phases with the same a value because of the very small chalcopyrite line splitting corresponding to the c/a value of 1.98. However for both the $z = 0.20$ and 0.25 samples, a value of the lattice parameter a for the single-phase condition was obtained and these are shown in Fig. 2. Another sample with $z = 0.20$ was sealed in a tube of thinner wall and similarly treated at 650°C. In this case, it was found that the quenched sample appeared to be single-phase chalcopyrite and again the a parameter obtained is shown in Fig. 2.

As is seen from Fig. 2, all of these values of a, whether for the chalcopyrite or zinc blende phase, lie within the limits of experimental error on a straight line which extrapolates to a value of $a = 0.6335$ nm at $z = 1.0$. This is in good agreement with the corresponding values obtained previously for the $(CuIn)_{1-z}Mn_{2z}Te_2$ (*7*) and $(AgIn)_{1-z}Mn_{2z}Te_2$ (*8*) alloys. In those cases also, there was no discontinuity in the a vs z line at the boundary between chalcopyrite and zinc blende phases. Using this line showing the variation of a with z, the limit of solid solubility in the chalcopyrite α phase at 200°C can be determined. For Fig. 2 this limit is seen to lie between $z = 0.03$ and 0.04. A sample annealed at 500°C gave a slightly higher value of about 0.05. These points are shown in the $T(z)$ diagram in Fig.

1. Because of the single-phase chalcopyrite form of one of the $z = 0.20$ samples, it is assumed that the α phase must extend beyond $z = 0.20$ in the vicinity of 600°C and thus the boundary between the α and $(\alpha + \gamma)$ fields has been drawn as shown in Fig. 1. One further result is that in the initial work, samples with $z = 0.50$ and 0.60 were annealed at 750°C and air quenched. These showed two-phase $(\beta + \gamma)$ form and the values of lattice parameter a for the β phase are given in Fig. 2. While these parameters cannot give a value for the composition of the β phase since the $(\beta + \gamma)$ field cannot satisfy pseudobinary conditions, the a values are consistent with a limit of the β phase in the vicinity of $z = 0.4$.

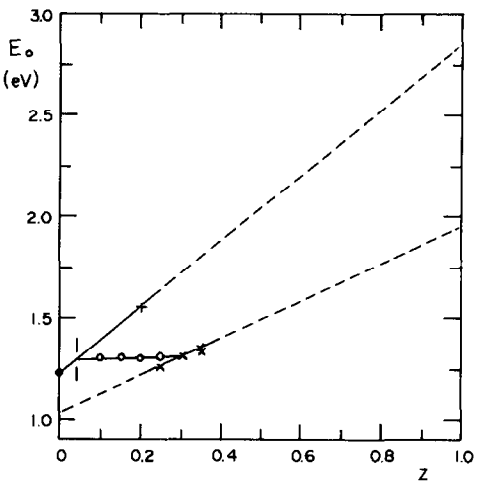

FIG. 3. Optical energy gap E_0 vs z for $(Cu Ga)_{1-z}Mn_{2z}Te_2$ alloys. Slowly cooled samples: ○, chalcopyrite. Quenched from 650°C: +, chalcopyrite; ×, zinc blende.

Optical Energy Gap Results

As has been indicated above, it is not possible from X-ray powder photograph data to determine whether a given sample is Mn-ordered or Mn-disordered. However in previous work on alloys of this type (*7, 8, 12*), it was shown that the values of optical energy gap E_0 are very useful as an indication of whether Mn-ordering is present in the alloy. It was found in all cases that a linear variation of E_0 with z is obtained but that the aiming point of the line at $z = 1.0$ is characteristic of the structure concerned. Thus, this value is 2.85 eV for the Mn-disordered zinc blende β phase, 1.95 eV for the Mn-ordered zinc blende β' phase, and 1.35 eV for the Mn-ordered chalcopyrite α' phase. In the case of the Mn-disordered chalcopyrite α phase, insufficient data were obtained to give a good value, the estimates varying from 2.85 (*8*) to 2.25 eV (*12*). The use of E_0 measurements in the present case is limited by the fact that many of the samples to be used may be multiphase. For optical absorption measurements on samples with more than one phase present, usually only the lowest energy gap is observed, the effects of the other phases occurring at absorption values too large to be measured. This is particularly the case with polycrystalline samples, such as those used in the present work, since if attempts are made to produce optical sample with thickness less than about 50 μm, the samples tend to crumble and disintegrate.

In the present work, E_0 measurements on samples showing from the X-ray results mainly the two-phase $(\alpha + \gamma)$ form gave E_0 values as shown in Fig. 3 which confirmed the X-ray data indicating a limit of solid solubility in the α field of $z = 0.04$. The single-phase chalcopyrite sample with $z = 0.20$ gave the value of $E_0 = 1.55$ eV shown in Fig. 3. A line drawn from the E_0 for Cu $GaTe_2$ ($z = 0$) through this point gives an aiming point at $z = 1.0$ of 2.85 eV. This would appear to indicate that this sample has the Mn-disordered chalcopyrite structure and reinforces the suggestion that the aiming point for Mn-disordered chalcopyrite is 2.85 eV. For the $z = 0.20$ multiphase sample, the only absorption edge observed gave a value of $E_0 = 1.29$ eV, correspond-

ing to the equilibrium chalcopyrite in the (α + γ) field. However, for the z = 0.25 sample, in addition to this edge a small absorption edge was observed corresponding to E_0 = 1.27 eV for a high-temperature phase. Finally, for the quenched samples with z = 0.30 and 0.35, which appeared cubic in the X-ray photographs, energy gap values were obtained as shown in Fig. 3. A line through these values at z = 0.25, 0.30, and 0.35 extrapolates at z = 1.0 to 1.95 eV indicating that these samples have the Mn-ordered zinc blende structure. The presence of Mn-ordered zinc blende structure in this diagram will be discussed further after the magnetic susceptibility results are given. If this cubic line is extrapolated to z = 0, a value of E_0 = 1.03 eV is obtained, which can be taken as the value for Cu $GaTe_2$ in the zinc blende form. In previous work (*11, 12*), similar extrapolations were made for $CuInTe_2$, $AgInTe_2$, and $AgGaTe_2$. In all cases, it is found that the difference between the measured gap of the chalcopyrite compound and that extrapolated for the zinc blende form is about 0.20–0.25 eV.

Magnetic Susceptibility Results

As was shown previously (*15*), a graph of magnetic susceptibility χ vs temperature T for these types of materials will show a cusp at the magnetic transition temperature T_m, which may correspond to a spin-glass–paramagnetic or to an antiferromagnetic–paramagnetic transition. As in the optical energy gap case, for a given composition the value of T_m will depend upon the phase condition of the sample, so that measurements of this type can be used to show the presence of Mn-ordered or Mn-disordered phases. However, these measurements have an advantage over those of E_0, in that if several different phases are present, it should be possible to observe a value of T_m corresponding to each. Thus this gives a very useful method for investigating the various phases produced by rapid quenching.

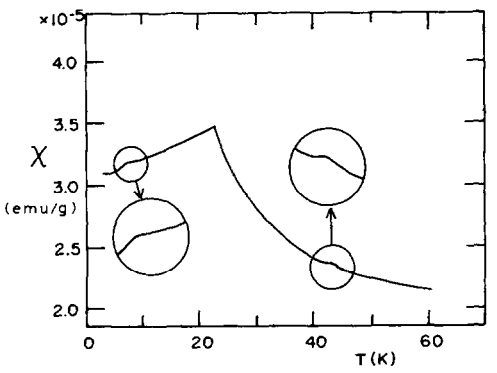

FIG. 4. Magnetic susceptibility χ vs temperature T for the alloy with z = 0.35 water quenched from 650°C.

This is illustrated by the curve of χ vs T (shown in Fig. 4) for the z = 0.35 sample annealed at 650°C and water quenched, which appeared to be single-phase cubic in the X-ray photograph. It is seen that the major cusp in the curve occurs at 23 K, but also small subsidiary peaks are observed at 43 and 9 K. In addition, there is probably a very small peak at 4–5 K but this at the lower limit of the available temperature range. These peak temperatures T_m are shown in Fig. 5 together with the corresponding values from other quenched samples. It is seen that the points fall on four separate lines, which as shown previously (*9*) can be attributed, in descending order of T_m, to Mn-ordered chalcopyrite, Mn-ordered zinc blende, Mn-disordered zinc blende, and Mn-disordered chalcopyrite. As obtained previously (*9*), the lines indicate a nearest-neighbor percolation limit of z = 0.19 for the face-centered cubic zinc blende and a value of z = 0.13 for the tetragonal chalcopyrite structure.

These results, together with those of optical energy gap measurements, indicate that samples water quenched from the single-phase zinc blende β field at 650°C can contain some amount of all of the four possible single-phase structures at the particu-

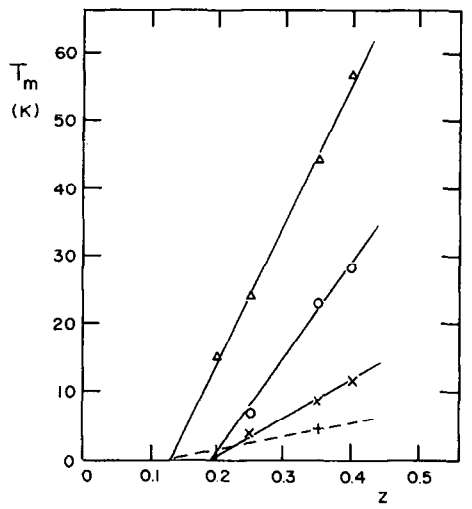

FIG. 5. Values of magnetic transition temperature T_m vs z for $(CuGa)_{1-z}Mn_{2z}Te_2$ alloys. △, Mn-ordered chalcopyrite; ○, Mn-ordered zinc blende; ×, Mn-disordered zinc blende; +, Mn-disordered chalcopyrite.

lar value of z. From the size of the peak in the χ vs T curve, it is clear that the cubic material in the samples is mainly Mn-ordered with a small amount of Mn-disordered material. However, the χ data indicate that in addition, even at $z = 0.35$, there is a small amount of the Mn-ordered chalcopyrite phase and probably a still smaller amount of the Mn-disordered chalcopyrite phase.

It is of interest to note that the equilibrium diagram contains no Mn-ordered cubic phase and probably no Mn-ordered chalcopyrite phase. It would appear that for a sample with Mn concentration z, with rapid quenching from the Mn-disordered cubic phase at 650°C, there is insufficient time for two-phase segregation to occur since this would involve long-range diffusion. Thus a metastable cubic phase of Mn concentration z is produced. However, it appears that during the quenching there is sufficient time for the Mn to order so that the major phase observed is Mn-ordered zinc blende with a small amount of zinc blende that did not manage to order. However, it is of interest that a small amount of chalcopyrite phase of Mn concentration z is observed. In the case of the $(AgGa)_{1-z}Mn_{2z}Te_2$ system, where single-phase behavior is obtained out to $z = 0.55$, it is found that in the range $0.35 \leq z \leq 0.55$ there is a transition from zinc blende to chalcopyrite at about 250°C. Thus the present magnetic data would perhaps indicate that for the $(CuGa)_{1-z}Mn_{2z}Te_2$ case, the chalcopyrite form is again a lower energy state than zinc blende at low temperatures, but that in this case the equilibrium condition is two-phase ($\alpha + \gamma$).

Conclusion

The results obtained here show that in contrast to the $(CuIn)_{1-z}Mn_{2z}Te_2$ (*10, 11*), $(AgIn)_{1-z}Mn_{2z}Te_2$ (*11*), and $(AgGa)_{1-z}Mn_{2z}Te_2$ (*12*) diagrams, in the $(CuGa)_{1-z}Mn_{2z}Te_2$ alloys the range of single-phase solid solution at room temperature is very small, being $0 \leq z \leq 0.04$ in the chalcopyrite phase and zero in the zinc blende phase. Only for temperatures of 600°C and above is a wide range of single-phase behavior obtained. One result of this, again in contrast with the other chalcopyrite alloys, is that no phases showing manganese ordering are observed in the equilibrium $T(z)$ section. However the magnetic susceptibility and optical energy gap data show that samples water quenched from the single-phase zinc blende field at 650°C consist mainly of Mn-ordered zinc blende material with small amounts of Mn-disordered zinc blende and Mn-ordered chalcopyrite phases present. Thus the optical energy gap and magnetic behavior of Mn-ordered samples can be investigated up to $z = 0.4$ by using these rapidly quenched metastable samples. The results are found to show good agreement with those previously obtained for other chalcopyrite-derived alloys.

Acknowledgments

The Venezuelan authors thank Consejo de Desarrole Cientifico Humanistico y Tecnologico (CDCHT) Venezuela for financial support.

References

1. J. K. FURDYNA, *J. Appl. Phys.* **53,** 6737 (1982).
2. J. A. GAJ, *J. Phys. Soc. Japan* **49,** 797 (1980).
3. R. R. GALAZKA, *Inst. Phys. Conf. Ser.* **43,** 133 (1979).
4. J. MYCIELSKI, *Prog. Cryst. Growth Charact.* **10,** 101 (1985).
5. R. BRUN DEL RE, T. DONOFRIO, J. E. AVON, J. MAJID, AND J. C. WOOLLEY, *Nuovo Cimento Soc. Ital. Fis. D* **2,** 1911 (1983).
6. T. DONOFRIO, G. LAMARCHE, AND J. C. WOOLLEY, *J. Appl. Phys.* **57,** 1932 (1985).
7. M. QUINTERO, L. DIERKER, AND J. C. WOOLLEY, *J. Solid State Chem.* **63,** 110 (1986).
8. M. QUINTERO AND J. C. WOOLLEY, *Phys. Status Solidi A* **92,** 449 (1985).
9. J. C. WOOLLEY, G. LAMARCHE, A. MANOOGIAN, M. QUINTERO, L. DIERKER, M. AL-NAJJAR, D. PROULX, C. NEAL, AND R. GOUDREAULT, *in* "Proceedings, 7th International Conference on Ternary and Multinary Compounds," p. 479, Materials Research Society (1987).
10. A. ARESTI, L. GARBATO, A. GEDDO-LEHMAN, AND P. MANCA, *in* "Proceedings, 7th International Conference on Ternary and Multinary Compounds," p. 497, Materials Research Society (1987).
11. M. QUINTERO, P. GRIMA, R. TOVAR, G. S. PEREZ, AND J. C. WOOLLEY, *Phys. Stat. Sol. (A)* **107,** 690 (1988).
12. M. QUINTERO, R. TOVAR, M. AL-NAJJAR, G. LAMARCHE, AND J. C. WOOLLEY, *J. Solid State Chem.* **75,** 136 (1988).
13. R. CHEN AND Y. KIRSH, "Analysis of Thermally Stimulated Processes" (Int. Series on Sci. Solid State, Vol. 15), p. 97, Pergamon, Elmsford, NJ (1981).
14. R. G. GOODCHILD, O. H. HUGHES, S. A. LOPEZ-RIVERA, AND J. C. WOOLLEY, *Canad. J. Phys.* **60,** 1096 (1982).
15. T. DONOFRIO, G. LAMARCHE, AND J. C. WOOLLEY, *J. Appl. Phys.* **57,** 1937 (1985).
16. A. CONGIU, L. GARBATO, AND P. MANCA, *Mater. Res. Bull.* **8,** 293 (1973).